

# Effect of Organic and Inorganic Ions on Lower Critical Solution Transition and Aggregation of PNIPAM

Leonor Pérez-Fuentes,<sup>†</sup> Delfi Bastos-González,<sup>\*,†</sup> Jordi Faraudo,<sup>‡</sup> and Carlos Drummond<sup>\*,¶,§</sup>

<sup>†</sup>*Biocolloid and Fluid Physics Group, Department of Applied Physics, University of Granada, Av. Fuentenueva 2, E-18001 Granada, Spain*

<sup>‡</sup>*Institut de Ciència de Materials de Barcelona (ICMAB-CSIC), Campus de la UAB, E-08193 Bellaterra, Barcelona, Spain*

<sup>¶</sup>*CNRS, Centre de Recherche Paul Pascal (CRPP), UMR 5031, F33600, Pessac, France*

<sup>§</sup>*Université de Bordeaux, CRPP, UMR 5031, F-33600 Pessac, France*

E-mail: dbastos@ugr.es; drummond@crpp-bordeaux.cnrs.fr

## Abstract

We have studied the effect of different ions belonging to the extended Hofmeister series on the thermosensitive polymer Poly (N-isopropylacrylamide) (PNIPAM), by combining Differential Scanning Calorimetry (DSC) and Dynamic Light Scattering (DLS). The variations in Lower Critical Solution Temperature ( $T_{LCS}$ ) and enthalpy change during PNIPAM phase separation evidences the importance of considering both hydration and hydrophobicity to explain the interaction of ions with interfaces. The results obtained in presence of inorganic ions can be explained by the tendency of water molecules to preferentially hydrate the PNIPAM chains or the ions, depending on the kosmotropic (highly hydrated) or chaotropic (poorly hydrated) character of the ions. On the contrary, tetraphenyl organic ions ( $\text{Ph}_4\text{B}^-$  and  $\text{Ph}_4\text{As}^+$ ) interact with the hydrophobic moieties of

PNIPAM chains, inducing a significant reduction of the  $T_{LCS}$ . DLS results show that the aggregation state of PNIPAM above the  $T_{LCS}$  is also strongly influenced by the presence of ions. While macroscopic phase separation (formation of a polymer-rich phase insoluble in water) was apparent in presence of inorganic ions, we observed the formation of submicron PNIPAM aggregates at temperatures above the  $T_{LCS}$  in presence of the hydrophobic ions. Kinetically arrested monodisperse PNIPAM nanoparticles were formed in presence of the  $\text{Ph}_4\text{B}^-$  anion, while a rather polydisperse distribution of particle sizes was observed in presence of  $\text{Ph}_4\text{As}^+$ . These results show that ionic specificity influences both the static (thermodynamic) and dynamic (kinetically controlled aggregation) state of PNIPAM in aqueous environment.

## Introduction

Poly (N-isopropylacrylamide) (PNIPAM) is a thermoresponsive polymer, containing hydrophilic and hydrophobic moieties. Its dissolution in water is favored by the possibility of hydrogen bonding between the amide groups in the polymer and water, which lowers the free energy of the binary system.<sup>1</sup> However, this bonding implies an entropic penalty to the mixing process due to its orientational nature. In addition, the presence of hydrophobic groups on the polymer also reduces the orientational freedom of nearby water molecules. As temperature is raised, the entropic contribution to the free-energy augments, decreasing the quality of water as PNIPAM solvent; at a particular temperature the entropic penalty dominates over the exothermic hydrogen bonding, and phase separation occurs.<sup>1,2</sup> Interestingly, this temperature is largely independent of polymer concentration; for this reason it is commonly termed lower critical solution temperature ( $T_{LCS}$ ), a term which strictly applies to the minimum of the coexistence curve.<sup>3</sup>

When  $T > T_{LCS}$ , several scenarios can be considered, depending on polymer concentration. The competition between intrachain contraction and interchain association (driven by

hydrogen bonding, van der Waals and hydrophobic interactions between a single or independent polymer chains) will determine the resulting state. Single chain coil-to-globule transition has only been observed at extremely low PNIPAM concentration.<sup>4,5</sup> At concentrations well below the overlapping concentration (dilute regime) microscopic phase separation has been reported: aggregation of colloidal particles of narrow size distribution has been observed by few research groups.<sup>6,7</sup> The size of the aggregates varied with heating history (rate and temperature) and polymer concentration, evidencing the out-of-equilibrium state of the colloidal system. It appears that the aggregates are stabilized by charges in the end-groups,<sup>8</sup> although other stabilization mechanisms related to low collision frequency in very diluted samples,<sup>9</sup> polymer chain self-organization (with the polar moieties oriented toward the aqueous continuous)<sup>10</sup> and low aggregation efficiency of colliding particles (due to viscoelastic effects)<sup>7</sup> have also been suggested. A detailed discussion on mesoglobule formation and kinetically arrested demixing in PNIPAM solutions was reported by Halperin and coworkers.<sup>11</sup> Colloidal stability has also been achieved by adding surfactants (e.g. SDS) to the water-PNIPAM mixture.<sup>12,13</sup> Finally, at sufficiently large polymer concentrations (in the semidilute or concentrated regimes) the interchain interaction largely dominates and macroscopic phase separation (precipitation) is observed. Most of the results presented in this paper correspond to the semidilute polymer concentration regime.

The balance between stabilizing and destabilizing factors in aqueous PNIPAM solutions is delicate; for instance, if any salt is added to the system, it may be anticipated that the hydrated ions will compete with the water around the hydrophobic and hydrophilic groups of the PNIPAM, reducing the  $T_{LCS}$ .<sup>14,15</sup> The distinctive impact of the interactions of salts (ions) with macromolecules is the origin of ionic specificity or Hofmeister effects.<sup>16</sup> It is often observed that ions interact with interfaces in a consistent way that cannot be explained by classical theories of colloidal interactions. A number of ions have been classified in the so-

called Hofmeister or lyotropic series (HS), which usually includes only inorganic ions. More recently this series has been extended to include some organic ions.<sup>17</sup> Although the origin of ionic specificity is still matter of debate, it is widely accepted that the position of the ions in the HS depends on the ionic hydration degree.<sup>18,19,17</sup> In this sense, poorly hydrated ions are usually referred as chaotropes while well hydrated ions are known as kosmotropes. Recently, some big molecular ions have been termed as soft matter disruptors<sup>20</sup> or super-chaotropes<sup>21,22</sup> as they show a behavior beyond the classical HS. These ions, located at the extreme positions in the HS, show strong interactions with hydrophobic matter and are able to solubilize hydrophobic molecules in aqueous media. Some examples are dodecaborate divalent anions,<sup>23</sup> the hexafluorophosphate anion<sup>16</sup> and organic tetraphenyl ions.<sup>17,24,25,26</sup> Anions usually prompt more pronounced Hofmeister effects than cations, which has been ascribed to the difference in the structure of water hydrating anions and cations.<sup>27,28,29</sup> The characteristics of the interacting species are also important in Hofmeister effects. For example, it has been recognized that hydrophobic surfaces strongly interact with chaotropic ions while hydrophilic surfaces interact more strongly with kosmotropic ones.<sup>17,30,31</sup> In this regard, the solvency properties of PNIPAM-based systems described above make them ideal candidates to investigate ionic specificity. A number of studies in this direction have been reported. Schild and Tirrel<sup>32</sup> reported a qualitative different effect of the presence of chaotropic or kosmotropic ions on PNIPAM solutions. They observed that  $T_{LCs}$  falls with increasing concentrations of kosmotropic ions (salting-out), but it augments if chaotropic ions at low concentrations are added (salting-in). Interestingly, the influence of chaotropic species is non-monotonic: salting-out was observed at larger concentrations of chaotropic ions. Analogous results for PNIPAM chains were reported by Thorman<sup>33</sup> and Cremer and co-authors<sup>34</sup> and by Bastos and coworkers for modified (charged) PNIPAM chains.<sup>35</sup>

Differential scanning calorimetry (DSC) has often been employed to study the  $T_{LCs}$  and other thermodynamic parameters of PNIPAM phase transition.<sup>32,36,37</sup> Several DSC studies have investigated the role played by different ions in the HS in the phase transition of PNIPAM.<sup>33,38</sup> However, as far as we know, no DSC studies using super-chaotropic organic ions have been reported. The main goal of this work is to investigate ionic specific effects in the heat phase transition and aggregation of PNIPAM, comparing representative inorganic ions of the HS with relatively large hydrophobic ions. We have used two tetraphenyl ions  $\text{Ph}_4\text{As}^+$  and  $\text{Ph}_4\text{B}^-$ . Both ions are large and with very similar external chemical and electronic structure, with four phenyl rings responsible for the direct interaction of the ions with water, surfaces or interfaces (see Figure 1a).<sup>27</sup> It has been shown in previous studies that tetraphenyl anions interact more strongly with PNIPAM microgels than tetraphenyl cations.<sup>27</sup>

## Experimental

### Materials

All the products were of analytical grade and used as received. The salts used were purchased from Scharlau and Sigma Aldrich. The tetraphenyl salts were obtained from Sigma Aldrich: sodium tetraphenylborate (ref T25402) and tetraphenylarsonium chloride (ref T25305). Poly(N-isopropylacrylamide) (PNIPAM) ( $M_w=19000 - 30000$  g/mol) was purchased from Sigma-Aldrich (ref 535311). Water used in all experiments was double distilled and deionized (DDI) with a Milli-Q Water Purification System (Millipore).

## Differential Scanning Calorimetry (DSC)

A Differential Scanning Calorimeter (DSC) (TA Instruments Microcalorimeter Q2000) measures the temperature and heat flow associated with material transitions as a function of time and temperature.<sup>39,40,41</sup> The sample material is encapsulated in a pan (measuring cell) and an empty reference pan is placed on the thermoelectric disk surrounded by a furnace. When the temperature of the furnace is changed at a linear rate, heat is transferred to the sample and reference through the thermoelectric disk. The differential heat flow to the sample and reference is measured by area thermocouples using the thermal equivalent of Ohm's Law:

$$q = \Delta T / R \quad (1)$$

where  $q$  is the sample heat flow,  $\Delta T$  is the temperature difference between the sample and the reference and  $R$  is the resistance of the thermoelectric disk. Additionally,  $\Delta T$  depends on the heat capacity ( $C_p$ ) of the sample. Usually, the heat capacity per unit mass is represented in function of the temperature in the thermograms.

Neutral PNIPAM chains were dissolved in cold water (4°C) at 5.6% or 16.7% w/w. The samples were stirred during five hours at 4°C until the solutions were completely transparent. The salt solutions were prepared at 10-fold the desired concentration for the experiments. Afterwards, salts and PNIPAM solutions were mixed at 1:9 proportions at room temperature. In this way, the final solution contains PNIPAM at 5% or 15% w/w. At high ionic concentrations (100 mM of Ph<sub>4</sub>AsCl and 1 M of NaCl and NaSCN) the PNIPAM chains were dissolved directly in the salt solutions in a water-ice bath. In all the experiments, 9  $\mu$ l of the final solution was enclosed in a pan (measuring cell). Each sample was equilibrated at 10°C during 10 minutes. Then, the sample underwent a heating cycle from 10 to 50°C, followed by an equilibrium time of 10 minutes and a cooling cycle (50–10°C). The

temperature rate in the cycles was of 1°C/min.

We performed three different thermograms (heating-cooling cycles) in pure water (for 5% and 15% of PNIPAM) by reloading the measuring cell with fresh solution and these repeated measurements were used to calculate the standard deviations of the measured quantities. We have assumed that these values also represent the uncertainties measured with the rest of the salts.

The  $T_{LCS}$  was calculated from the onset temperature ( $T_{ons}$ ) of the endothermic peak determined as the intersection of the tangent of the endotherm's maximal slope and the baseline.  $T_{max}$  is the temperature at the maximum point of the endothermic peak (see Figure 2). The change in enthalpy ( $\Delta H$ ) during the process, was calculated from the area under of the endothermic peak.

## **Dynamic Light Scattering**

Dynamic light scattering (DLS) was performed on an ALV goniometer and a digital correlator ALV-5000 (laser wavelength 633 nm; scattering angles between 30 and 145°). Particle sizes were determined from the measured intensity autocorrelation function of the scattering intensity using the method of cumulants.<sup>42</sup>

PNIPAM/salt solutions were prepared at room temperature. For aging and particle size measurements, 2.5 ml of polymer solution were placed in borosilicate glass tubes (100 mm length, 1 mm wall thickness; VWR) and stored at 25°C before measurement. PNIPAM aggregation was triggered by placing the tubes in a large size bath at 45°C. Samples were aged at least 30 minutes before carrying out DLS measurements.

## Results and discussion

We have studied the thermally induced phase transition of PNIPAM by differential scanning calorimetry (DSC) and dynamic light scattering (DLS). DSC allows studying the thermodynamic parameters of the heat-induced phase transition. The polymer used in this work has a molecular weight,  $M_w$ , between 19 and 30 kDa. We can estimate its gyration radii,  $R_g$ , in good solvent conditions by extrapolation the results reported by Kubota and coworkers,<sup>43</sup> as  $R_g = 0.22M_w^{0.54}$  (nm). Using this expression, we obtain values of  $R_g$  between 4.5 and 5.8 nm. We can then estimate the polymer overlapping concentration in good solvent condition,  $C$ , as

$$C^* = \frac{3M_w}{4\pi N_A R_g^3} \quad (2)$$

Thus, for the PNIPAM used in this study,  $C^*$  varies between 6.3 and 8.3% w/w. Most of the results presented in this study were obtained at semidilute conditions ( $C > C^*$ ). Some tests in dilute conditions ( $C < C^*$ ) were also performed as indicated.

Figure 2 displays the measured relative specific heat for a solution of PNIPAM 15% w/w in pure water. One typical heating-cooling cycle obtained at a scan rate of 1°C/min is presented. The heat exchange in the transition,  $\Delta H$ , the  $T_{LCS}$  and the temperature at the peak of specific heat can be easily determined from the thermogram. As described above, the process is the result of the intrachain collapse of the PNIPAM chains around the  $T_{LCS}$  of the polymer and the interchain aggregation due to the high concentration of PNIPAM chains in the solution. The whole process is endothermic: heat must be added to the system to complete the transition. Early studies associated this fact to the rupture of polymer-solvent hydrogen bonds.<sup>32,44</sup> Other groups have attributed more importance to the hydrophobic



effect.<sup>45</sup> Although there is still some controversy about the exact mechanism controlling the transition, it is clear that the interplay of both effects determines the overall behavior of the system. We will come back to this point below.

As can be observed in Figure 2, the temperature at the maximum value of  $\Delta C_p$  is lower while cooling than in the heating step,  $\Delta T_{max} = 0.5^\circ\text{C}$ , indicating hysteresis in the cycle. We have consistently observed this difference between heating and cooling steps in all the measured thermograms. This hysteresis, which has been previously reported, is commonly attributed to additional hydrogen bonding on PNIPAM chains formed in the collapsed state.<sup>4,46,47</sup> However, when the temperature is decreased enough the system comes back to its original state.<sup>46,47</sup>

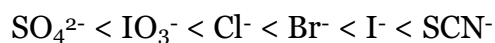
We have studied the influence of a number of different anions on the  $T_{LCS}$ , in order to cover a representative range from kosmotropic to chaotropic anions in the HS. These results will be compared to those obtained with the organic super-chaotropic ions, tetraphenylarsonium ( $\text{Ph}_4\text{As}^+$ ) and tetraphenylborate ( $\text{Ph}_4\text{B}^-$ ). Thermograms measured in presence of the reference salt, NaCl, and for the most chaotropic inorganic salt investigated, NaSCN, are presented in Figure 3. For the case of NaCl, increasing salt concentration results in a monotonic decrease of  $T_{LCS}$ . At 10 mM no significant effect on  $T_{LCS}$  is observed (in comparison with pure water). On the contrary, at 100 mM and 1 M the reduction of  $T_{LCS}$  can be clearly observed. A different behavior is observed in the presence of NaSCN:  $T_{LCS}$  increases at 100 mM, and slightly decreases at 1 M. Given that both salts share the same cation,  $\text{Na}^+$ , their dissimilar effect must be attributed to the anions. The influence of NaCl could be anticipated: given that this salt shows more affinity for water than PNIPAM, as the concentration of  $\text{Cl}^-$  increases the polymer dehydrates more easily, reducing the  $T_{LCS}$ . The same idea can be expressed differently: NaCl is partially excluded from the PNIPAM-

water interface, destabilizing the macromolecule by increasing its chemical potential. This effect promotes the reduction of the effective area of contact between the polymer and the solvent, favoring the collapse of the macromolecule. As  $\text{SCN}^-$  is a poorly hydrated anion, it seems reasonable that it prompts a poorer dehydrating effect: it is necessary to add a high concentration of  $\text{SCN}^-$  to observe a  $T_{LCS}$  slightly lower than the value obtained in pure water. The reasons behind the increment of  $T_{LCS}$  at moderate  $\text{SCN}^-$  concentrations are less intuitive. This behavior, repeatedly observed in the past, has been attributed to the favorable interaction between the poorly hydrated anion and the collapsed polymer chains, which stabilizes the polymer chains in solution.

As can be observed in Figure 3, the effect of ions goes beyond a shift in  $T_{LCS}$ ; the general shape of the PNIPAM endothermic curves is also clearly changed. For the case of NaCl this change is observed at 1 M: the heat capacity curve is broader and its height is clearly reduced in comparison with lower NaCl concentrations (Figure 3a). On the other hand, for the case of NaSCN, the curve clearly changes at 100 mM, becoming broader; this effect is even more pronounced at 1 M (Figure 3b). The changes in the curves indicate that the balance collapse/aggregation of the PNIPAM chains is being affected by the type and concentration of salt. Similar results were reported by Shechter *et al.* in a study of PNIPAM in presence of KSCN.<sup>38</sup> They argued that in pure water the PNIPAM collapse occurs in a sharp transition due to the cooperative collapse of long segments and probably of the entire polymer chains.<sup>32</sup> On the contrary, when salt is present the collapse is a less cooperative process because the  $\text{SCN}^-$  bound to PNIPAM reduces the length of unperturbed segments of the chains. Hence, the size distribution heterogeneity of the chains increases, resulting in decreasing the peak height and increasing its width. We will return to this point later.

Next, we measured the thermograms for a number of inorganic salts representative of the HS.

Table 1 shows the results obtained with these inorganic ions. As expected, the  $T_{LCS}$  and  $T_{max}$  values depend on the type and concentration of salt. Figure 4 shows the thermograms for the different salts at 100 mM. The values of the  $T_{LCS}$  follow the sequence:



which corresponds to the reverse HS. More hydrated anions induce lower  $T_{LCS}$  values in PNIPAM because of their higher affinity for water. On the contrary, in presence of more chaotropic anions water prefers to hydrate the polymer. For the combination of effects described before, an increment in  $T_{LCS}$  is observed in presence of  $\text{I}^-$  and for the poorly hydrated  $\text{SCN}^-$  anion. The dissimilar influence of kosmotropic and chaotropic ions can be further assessed by examining the correlation between the hydration of the anions and the response of PNIPAM to temperature changes. As can be observed in Figure 4b, while the change in  $T_{max}$  appears to correlate well with the enthalpy of hydration of the well-hydrated (kosmotropic) anions,<sup>48</sup> the correlation is lost for the case of  $\text{SCN}^-$ .

The reduction of  $T_{LCS}$  by highly and moderate hydrated anions and the opposite effect by poorly hydrated anions have been previously observed by other authors working with neutral PNIPAM chains<sup>15</sup> and charged PNIPAM chains and microgels.<sup>35,49</sup> In a series of papers lead by Cremer, the increase on the  $T_{LCS}$  for the most chaotropic anions was attributed to anionic binding to the amide moieties (NH group) of PNIPAM, which would cause the charge of the polymer surfaces.<sup>34</sup> However, in a more recent study of Poly(N,N-diethylacrylamide) (PDEA) Cremer and co-authors have found that the NH group is not required for the interactions between weakly hydrated anions and polymer chains in aqueous solutions. They concluded that only the backbone CH groups provide a binding site for the weakly hydrated anions.<sup>50</sup> A similar conclusion was reached by Bastos and coworkers in a previous study of modified (charged) PNIPAM chains.<sup>35</sup> This hypothesis is supported by the

recent report that poly(propylene oxide) (PPO), which has no amide groups in its structure, also increases its phase separation temperature in comparison to pure water in presence of KSCN.<sup>33</sup>

It can also be observed in Figure 4 that the height and width of the DSC peaks depend on the type of salt employed: the height decreases and the width increases as the anion is more kosmotropic. Interestingly, a similar effect is observed for the most chaotropic ion,  $\text{SCN}^-$ . Schild and Tirrell observed very similar tendencies in the calorimetric peaks working with PNIPAM chains and  $\text{Na}_2\text{SO}_4$ , NaSCN and NaBr; they pointed out that the physical origin of the  $T_{LCS}$  changes must be different for each salt.<sup>32</sup> We propose that these discrepancies are a consequence of the dissimilar interaction of these ions with hydrophobic surfaces. When  $T_{LCS}$  is surpassed, PNIPAM globules and aggregates contain significantly more hydrophobic internal environments.<sup>51</sup> As mentioned above, kosmotropic anions are excluded from hydrophobic interfaces while chaotropic ones are accumulated on them.<sup>30,52</sup> Thus, at temperatures below  $T_{LCS}$  kosmotropic anions weaken the interaction between water and PNIPAM possibly turning the cooperative collapse of the PNIPAM chains more heterogeneous, which would imply wider peak transitions. As kosmotropic anions tend to be excluded from the interface, the final state reached for the collapsed/aggregated PNIPAM chains should be similar to the one reached in pure water. On the contrary, chaotropic anions feel a weak (but significant) attraction for the hydrophobic patches of PNIPAM interfaces and will tend to accumulate on them. This effect is especially relevant for the most chaotropic anion,  $\text{SCN}^-$ , which has been previously showed to be able to reverse the surface charge of PNIPAM cationic microgels and PNIPAM charged chains at low concentrations.<sup>35,49</sup> As the temperature gets closer to the  $T_{LCS}$ ,  $\text{SCN}^-$  increasingly interacts with PNIPAM chains and aggregates, enhancing their stability in water. This effect could have a limited extension: after the interaction sites are

occupied, further salt addition will probably exert an effect due to excluded volume, reducing  $T_{LCS}$ . This effect could decrease the cooperativity of the transition, which is probably the reason for the observed increase of the width of the DSC peak. It is important to emphasize that when the ions have a favorable interaction with the polymer the final state of the globules and aggregates will be different from the ones in pure water, because of the accumulation of the poorly hydrated anions in the aggregates.

The dissimilar behavior between kosmotropic and chaotropic ions is supported by the change of enthalpy during the transition,  $\Delta H$ , which was measured from the integration of the endothermal peak. We can see in Table 2 that  $\Delta H$  remains almost constant for all the inorganic salts except for the  $SCN^-$ . This suggests that the mechanism PNIPAM changes its hydration is independent of the nature of the salt present in the medium with the exception of  $SCN^-$ , indicating that this ion interacts with PNIPAM in a different or more extensive way than the other anions, and that it is able to significantly alter the dehydration of the polymer. In an analogous study with poly(propylene oxide) (PPO), Thormann<sup>33</sup> reported that  $\Delta H$  only was significantly reduced with increasing salt concentration for KSCN while for the rest of the salts it remained almost unaffected. He ascribed this result to a decrease of the hydrophobic hydration of PPO by the KSCN, which agrees with the mechanism proposed by us.

Next, we are going to describe the thermograms obtained in the presence of the tetraphenyl ions. As mentioned in the Introduction these ions have similar size and the same external chemical structure (Figure 1a). Because of their hydrophobic character, we would expect a behavior similar to the one observed with the most poorly hydrated inorganic anions for both the  $Ph_4B^-$  and the  $Ph_4As^+$ . These hydrophobic ions should not compete with the water hydrating PNIPAM and they strongly interact with hydrophobic moieties of the polymer, which should be reflected in a slightly increase of  $T_{LCS}$  at low or moderate concentration

of salt and a decrease when the concentration is increased. Results are shown in Figures 5 and 6 and Tables 3 and 4 for two PNIPAM solutions at 15% and 5% w/w, respectively.

Figure 5a shows the thermogram for the  $\text{Ph}_4\text{B}^-$  at three different salt concentrations. It was not possible to obtain thermograms at higher  $\text{Ph}_4\text{B}^-$  concentrations due to the precipitation of the PNIPAM chains in solution. We can see that in spite of the extremely low salt concentrations used,  $T_{LCS}$  diminishes as the concentration is increased (cf. Table 3), while the height of the peaks decreases and the curves become wider. This ionic effect at low salt concentrations is quite remarkable: ionic specificity is typically observed at much larger concentrations (at least a few tens of mM). In addition, this behavior is not in accordance with that observed for other poorly hydrated inorganic anions (e.g.  $\text{SCN}^-$ ). It is clear that there is a strong interaction between the  $\text{Ph}_4\text{B}^-$  anion and PNIPAM even at very low concentrations and at temperatures below  $T_{LCS}$ . In contrast, the results with  $\text{Ph}_4\text{As}^+$  (Figure 5b) shows that the  $T_{LCS}$  tends to increase in the concentration range studied, in accordance with the results found for the most chaotropic inorganic anion ( $\text{SCN}^-$ ). We have to limit our study to a maximum value of  $\text{Ph}_4\text{As}^+$  concentration of 100 mM because of its limited solubility. For this reason we did not observe a subsequent fall in  $T_{LCS}$ , as was the case for the inorganic anions. A very strong interaction between these ions and PNIPAM (chains and microgels) and the dissimilar behavior for  $\text{Ph}_4\text{B}^-$  and  $\text{Ph}_4\text{As}^+$  have been previously reported by us.<sup>27</sup> Molecular dynamic simulations with PNIPAM chains, showed that both ions strongly interact with the isopropyl group of the PNIPAM but while  $\text{Ph}_4\text{B}^-$  preferentially interacts with the methyl ( $-\text{CH}_3$ ) and the backbone methylene ( $-\text{CH}_2$ ) groups of PNIPAM,  $\text{Ph}_4\text{As}^+$  has a stronger interaction with the methyl ( $-\text{CH}_3$ ) and the oxygen atom of the amide ( $-\text{CONH}$ ) groups (see Figure 1). This difference makes the interaction of  $\text{Ph}_4\text{B}^-$

with PNIPAM stronger than the one of  $\text{Ph}_4\text{As}^+$ . In reference 19 we evaluated the strength of this interaction, obtaining values of  $-37.7$  kcal/mol for the  $\text{Ph}_4\text{B}^-$  and  $-8.5$  kcal/mol for the  $\text{Ph}_4\text{As}^+$ . In the case of inorganic cations, other studies show that the interaction of PNIPAM amide groups is significant for a small cation, such as  $\text{Li}^+$ , but it is weak for a larger cation  $\text{Cs}^+$ , and divalent cations ( $\text{Ca}^{2+}$ ,  $\text{Mg}^{2+}$ ).<sup>53</sup> We have found that  $\text{Na}^+$  interacts with PNIPAM amide group but this interaction is not strong enough to lead adsorption of  $\text{Na}^+$  on PNIPAM.<sup>27</sup> From the different results it becomes clear that the size of the cation is not the determinant factor in the interaction of PNIPAM amide-cation. Simulation results suggested that although the hydrophobic effect plays a fundamental role in the PNIPAM tetraphenyl ion interactions, the structural details of the  $\text{Ph}_4\text{B}^-$ -PNIPAM and  $\text{Ph}_4\text{As}^+$ -PNIPAM interactions are different.<sup>27</sup> The experimental results obtained by DSC confirm these observations.

Given the limited solubility of the hydrophobic salts, we measured thermograms at a lower PNIPAM concentration 5% to investigate the effect of larger salt/polymer ratios in the critical solution transition. We found the same general trends observed at 15%, but the influence of the anion for similar PNIPAM/tetraphenyl ratios seems to be even more significant. At 0.07 mM of  $\text{Ph}_4\text{B}^-$  the  $T_{LCS}$  is similar to the value measured in the absence of salt (cf. Table 4) but the height and width of the curve are clearly changed, as a consequence of the interaction between  $\text{Ph}_4\text{B}^-$  and PNIPAM (Figure 6a). For larger salt concentrations the decrease of  $T_{LCS}$  is clearly observed; at 7 mM of salt the decrease on the  $T_{LCS}$  is around  $5^\circ\text{C}$ . In addition, the height of the curves is reduced and they become wider. At this low salt concentration none of the other anions, including the hydrophobic  $\text{Ph}_4\text{As}^+$ , would induce a significant variation in  $T_{LCS}$  (cf. Tables 1 and 3). These changes suggest a less homogeneous

collapse of the PNIPAM chains as the interaction with  $\text{Ph}_4\text{B}^-$  acquires more relevance. This interaction is so strong that it disturbs the PNIPAM structure, acting as a real disruptor of soft matter or super-chaotropic ion, as found in previous studies.<sup>27</sup>

The  $\text{Ph}_4\text{As}^+$  results on Figure 6b and Table 4 also confirm the tendency observed at 15% of PNIPAM. We observe a slight increment on  $T_{LCs}$  for larger salt concentrations, in marked contrast with the results obtained with  $\text{Ph}_4\text{B}^-$ . Even though both ions are almost identical in size and polarizability the way they interact with PNIPAM is clearly different, as reflected in the thermograms.

We have also measured  $\Delta H$  for the PNIPAM volume phase transition in presence of the hydrophobic ions (Tables 3 and 4). A significant  $\Delta H$  reduction was observed for both salts. This reduction seems to be largely independent of salt concentration for the case of  $\text{Ph}_4\text{B}^-$  specially at 5%, where the  $\Delta H$  reduction is observed at very low salt concentration, 0.07 mM and it remains constant until the maximum value tested of 14 mM. On the contrary, at 15% the  $\Delta H$  values tend to decrease as the concentration of  $\text{Ph}_4\text{As}^+$  increases, as was observed for the case of  $\text{SCN}^-$ . Indeed, the parallelism between the results obtained with  $\text{SCN}^-$  and  $\text{Ph}_4\text{As}^+$  is remarkable: it reflects that both ions strongly interact with PNIPAM in spite of their difference in charge sign, size and structure. Nevertheless, at 100 mM salt concentration the  $T_{LCs}$   $\text{Ph}_4\text{As}^+$  is 33.5°C, while for the  $\text{SCN}^-$  we found 34.5°C. This could be understood as a consequence of a larger influence of the poorly hydrated inorganic anion than that of  $\text{Ph}_4\text{As}^+$ . However, as we are changing both the cation and the anion, this comparison must be handled with caution. The big cation is clearly hydrophobic and we have previously shown that it interacts strongly with PNIPAM.<sup>27</sup> Indeed, subsequent results will show that the interaction of  $\text{Ph}_4\text{As}^+$  with PNIPAM is in fact stronger than that of



SCN<sup>-</sup>.

It is informative to compare the values of  $\Delta H$  measured during heating and cooling processes, as mentioned before, they can be significantly different (Figure 2). Ding *et al.* reported that the enthalpy change upon cooling was always smaller than in the heating process.<sup>46</sup> We observed a similar effect for all the conditions investigated. For instance, comparing heating versus cooling processes for 5% PNIPAM solution we found around 25% reduction in  $\Delta H$  when the heating-cooling cycle was measured in water or in presence of Ph<sub>4</sub>As<sup>+</sup>. Interestingly, we found a significant smaller reduction for the case of Ph<sub>4</sub>B<sup>-</sup> (between 2 and 8%). The dramatic effect of the ionic environment on the reversibility of a heating-cooling cycle can be appreciated in Figure 7. Similarly to what is observed in pure water, in presence of 10 mM of NaCl (Figure 7a) a substantial difference in the shape of the thermograms (heating vs. cooling) and a significant reduction in  $\Delta H$  can be appreciated. On the contrary, by adding a small amount Ph<sub>4</sub>B<sup>-</sup> (1 mM) the differences between heating and cooling process are largely reduced (Figure 7b). This substantial difference points to the possibility of significant change in the coil-globule transition in the latter case, suggesting that the detailed structure of the collapsed state will be very different in both cases. To further explore this matter, we carried out aggregation and DLS measurements.

The aggregation state of the PNIPAM solution in presence of the different salts is very revealing. As can be appreciated in the photographs presented in Figure 8 (taken after the samples were aged at T=45°C for 30 minutes), the turbidity of the system was clearly salt dependent, even though the mixing, aging process and thermal history were strictly identical in all cases. In the presence of Ph<sub>4</sub>B<sup>-</sup> a clear (bluish) appearance was observed. On the contrary, in presence of NaCl or NaSCN the PNIPAM solution became milky as soon as the  $T_{LCS}$  was surpassed. The 100 mM SCN<sup>-</sup> sample shows clear phase separation.

Figure 8b shows similar results for lower PNIPAM concentration. While highly turbid solutions were obtained in presence of NaCl or NaSCN, PNIPAM aggregation was clearly stopped in an earlier stage by adding the hydrophobic salts, suggesting the formation of submicrometric particles. It is important to emphasize that the polymer concentrations investigated in this work are larger than in most previous studies of mesoglobule formation in PNIPAM solutions (in particular for the samples presented in Fig. 8a), precluding the likelihood of low efficiency of collision as the mechanism responsible for the observed salt-dependent limited aggregation.<sup>11</sup>

We performed DLS measurements of the different samples at temperatures above the  $T_{LCS}$ . We have reduced PNIPAM concentration to 0.5% to minimize multiple scattering. As it can be inferred from the photographs in Figure 8, large particle size (and multiple scattering) was observed for NaCl or NaSCN. On the contrary, we observed the formation of long-lasting small particles with very narrow size distributions in presence of  $\text{Ph}_4\text{B}^-$ . The average particle radius varied from 20 to 100 nm (much larger than the expected size of single PNIPAM chains). In fact, the particle size can be tuned by the concentration of polymer chains and  $\text{Ph}_4\text{B}^-$ , as can be observed in Figure 9. The mean PNIPAM particle size initially decreases and then increases for progressively larger salt concentrations; this remarkable behavior is related to the association of the anion with the polymer aggregate. After being formed, the nanoparticles neither precipitated nor change their size for several days. Interestingly, the addition of an indifferent salt (e.g. NaCl) quickly destabilized the polymer aggregates, triggering macroscopic phase separation.

Some important questions arise: what is the mechanism responsible for the stability of these colloidal particles, and consequently what determines their limited size? We believe it can be linked to the mechanisms of control of particle size in the preparation of polymer

lattices or ionic microgels. The fact that the particles lose their stability at high salt concentrations indicates that electrostatic repulsion is at the origin of the stabilizing colloidal interactions, overcoming the strong tendency of the macromolecules to aggregate. This idea is clearly supported by the coalescence of the colloidal particles triggered by NaCl addition. It is apparent that the favorable interaction between the PNIPAM chains and the  $\text{Ph}_4\text{B}^-$  ions confers an effective electric charge to the growing polymer aggregates. Thus, it seems reasonable to expect that the number of charges associated to the growing colloidal particle will be proportional to the number of associated NIPAM monomers, and it will increase with tetraphenyl ion concentration (up to a given saturation limit). If we assume the formation of compact aggregates, the number of charges per aggregate will be proportional to its volume,  $\sim r^3$ , where  $r$  is the radii of the particle. As the effective area of the particle increases as  $r^2$ , the charge density of the particle,  $\sigma$ , will increase with the size  $r$  of the polymer aggregate, increasing the interparticle electrostatic repulsion and potentially limiting their coalescence, as effectively observed. As the polymer-ion interaction probably depends on the experimental conditions (e.g. thermal history or concentration), it is likely that the final size of the aggregates will depend on the details of the experimental protocol. This aspect will be further investigated in the future.

The dual effect of the added tetraphenyl salt on the stability of the PNIPAM aggregates can be easily grasped. On one hand, adding salt increases the value of  $\sigma$ , stabilizing the growing aggregate. On the other hand, increasing ionic strength enhances the screening of the electrostatic repulsion between the colloidal particles and reducing its stability. If the association constant of the polymer chains and the ions is sufficiently strong, the coalescence of forming polymer aggregates can be halted, and colloidal particles are formed.

For the case of  $\text{Ph}_4\text{As}^+$  it was necessary to further reduce the concentration of PNIPAM to limit polymer aggregation. We observed formation of particles with diameter of between 350 and 1500 nm at 0.005% PNIPAM and 10 mM of salt. With the other two salts, NaSCN and NaCl, we were not able to limit aggregation at any combination of PNIPAM and salt concentration. Even if there is a favorable interaction between the ionic species and the polymer chains (as is obviously the case for  $\text{SCN}^-$ ), it is not strong enough to promote a value of  $\sigma$  large enough to stabilize the colloidal aggregates. These results evidence that the interaction of the big tetraphenyl ions with the PNIPAM hydrophobic interface is stronger than that of the poorly hydrated inorganic anion  $\text{SCN}^-$ , and that the interaction of  $\text{Ph}_4\text{B}^-$  with PNIPAM is much stronger than for the case of  $\text{Ph}_4\text{As}^+$ .

The particle formation in the presence of strongly adsorbing salts can be associated with the reported formation of stable PNIPAM nano aggregates in presence of surface active agents<sup>54</sup> or charged monomers copolymerized with the PNIPAM<sup>55</sup>, as represented in Figure 10. The ions probably associate with the polymer due to hydrophobic interaction, preventing aggregation due to electrostatic stabilization. This process is fully reversible. Upon cooling, the particles disappeared at  $T < T_{LCS}$ . The limited PNIPAM aggregation at  $T > T_{LCS}$  may be the reason of the reduced  $\Delta H$  and the enhanced reversibility (Figure 7b) observed in presence of the hydrophobic or chaotropic salts. Particle formation limits the contribution of the hydrophobic interaction of the collapsed polymer chains, reducing the enthalpy change measured during the transition and enhancing its reversibility. Under the light of these results, it is apparent that the monotonic reduction of  $T_{LCS}$  induced by both kosmotropic ions and the super-chaotropic hydrophobic tetraphenyl anion  $\text{Ph}_4\text{B}^-$  have different causes. For the case of strongly hydrated ions the progressive reduction in PNIPAM solubility is due to excluded-volume effects; at high temperature the polymer chains are

dehydrated, but the ions do not form part of the aggregate formed. On the contrary, the hydrophobic anion interacts strongly with the chains and is associated within the aggregates of limited size. The aggregates are formed by collective binding in presence of the hydrophobic ion rather than by polymer exclusion.

## Conclusions

We have used DSC to study the influence of different salts on the Lower Critical Solution Transition of PNIPAM. The ionic influence varied according to the Hofmeister series. More hydrated anions (kosmotropic) dehydrate PNIPAM chains, reducing the  $T_{LCS}$  to a higher extension than less hydrated anions (chaotropic). In both cases the broadening of the range of the observed transition indicates that salt addition reduces its cooperativity.

The results obtained with the  $SCN^-$  point out that, in addition to water competition, this chaotropic anion interacts with the hydrophobic moieties of PNIPAM chains enhancing their solubility and increasing the  $T_{LCS}$  of the PNIPAM.

Calorimetric data confirm that the super-chaotropic ions strongly interact with PNIPAM. We found that the tetraphenyl anion interacts more strongly with the hydrophobic PNIPAM interface than the tetraphenyl cation. This difference has been reflected in the displacement of  $T_{LCS}$  for both salts: while  $Ph_4B^-$  significantly reduced the  $T_{LCS}$  at low concentrations,  $Ph_4As^+$  slightly increased the  $T_{LCS}$  in the range of concentrations studied. More importantly, the formation of long-lasting small particles with very narrow size distributions at temperatures higher than  $T_{LCS}$  was observed for the  $Ph_4B^-$  anion, but not for the  $Ph_4As^+$  cation or other inorganic salts. However, in presence of  $Ph_4As^+$  we could observe the formation of particles with polydisperse size distribution.

Finally, the results obtained for the most chaotropic anion  $SCN^-$  and those obtained for the

organic ions showed similar tendencies, which reinforces the conclusion that the origin of Hofmeister effects or ionic specificity are intimately linked to the hydration properties of both, ions and interacting surfaces.

## **Acknowledgement**

The authors thank the financial support granted by the project CTS-6270 (Junta de Andalucía, Spain) and the Spanish Ministerio de Economía y Competitividad, Plan Nacional de Investigación, Desarrollo e Innovación Tecnológica (I + D + i) (Project FIS2016-80087-C2-1-P). J.F. acknowledges financial support from the Spanish Ministerio de Economía y Competitividad, through the "Severo Ochoa" Programme for Centres of Excellence in R & D (SEV-2015-0496) awarded to ICMAB. L.P.-F. thanks the financial support provided by the COST Action MP1303: Understanding and Controlling Nano and Mesoscale Friction.

## References

- 1 H. G. Schild, *Prog. Polym. Sci.*, 1992, **17**, 163–249.
- 2 K. Shiraga, H. Naito, T. Suzuki, N. Kondo and Y. Ogawa, *J. Phys. Chem. B*, 2015, **119**, 5576–5587.
- 3 Y. Okada and F. Tanaka, *Macromolecules*, 2005, **38**, 4465–4471.
- 4 C. Wu and X. Wang, *Phys. Rev. Lett.*, 1998, **80**, 4092–4094.
- 5 X. Wang, X. Qiu and C. Wu, *Macromolecules*, 1998, **31**, 2972–2976.
- 6 M. H. Siu, C. He and C. Wu, *Macromolecules*, 2003, **36**, 6588–6592.
- 7 C. Wu, W. Li and X. X. Zhu, *Macromolecules*, 2004, **37**, 4989–4992.
- 8 K. Chan, R. Pelton and J. Zhang, *Langmuir*, 1999, **15**, 4018–4020.
- 9 A. V. Gorelov, A. Du Chesne and K. A. Dawson, *Phys. A Stat. Mech. its Appl.*, 1997, **240**, 443–452.
- 10 V. Aseyev, S. Hietala, A. Laukkanen, M. Nuopponen, O. Confortini, F. E. Du Prez and H. Tenhu, *Polymer (Guildf.)*, 2005, **46**, 7118–7131.
- 11 A. Halperin, M. Kröger and F. M. Winnik, *Angew. Chemie - Int. Ed.*, 2015, **54**, 15342–15367.
- 12 H. G. Schild and D. A. Tirrell, *Langmuir*, 1991, **7**, 665–671.
- 13 M. Meewes, J. Ricka, M. de Silva, R. Nyffenegger and T. Binkert, *Macromolecules*, 1991, **24**, 5811–5816.
- 14 T. López-León, J. L. Ortega-Vinuesa, D. Bastos-González and A. Elaïssari, *J. Phys. Chem. B*, 2006, **110**, 4629–4636.
- 15 Y. Zhang and P. S. Cremer, *Annu. Rev. Phys. Chem.*, 2010, **61**, 63–83.
- 16 P. Lo Nostro and B. W. Ninham, *Curr. Opin. Colloid Interface Sci.*, 2016, **23**, A1–A5.
- 17 D. Bastos-González, L. Pérez-Fuentes, C. Drummond and J. Faraudo, *Curr. Opin. Colloid Interface Sci.*, 2016, **23**, 19–28.
- 18 Y. Zhang and P. S. Cremer, *Curr. Opin. Chem. Biol.*, 2006, **10**, 658–663.
- 19 W. Kunz, *Curr. Opin. Colloid Interface Sci.*, 2010, **15**, 34–39.
- 20 E. Leontidis, M. Christoforou, C. Georgiou and T. Delclos, *Curr. Opin. Colloid Interface Sci.*, 2014, **19**, 2–8.
- 21 K. I. Assaf, M. S. Ural, F. Pan, T. Georgiev, S. Simova, K. Rissanen, D. Gabel and W. M. Nau, *Angew. Chemie Int. Ed.*, 2015, **54**, 6852–6856.
- 22 D. Bastos-González, L. Pérez-Fuentes, C. Drummond and J. Faraudo, *Curr. Opin. Colloid*

- Interface Sci.*, 2016, **23**, 19–28.
- 23 K. I. Assaf, M. S. Ural, F. Pan, T. Georgiev, S. Simova, K. Rissanen, D. Gabel and W. M. Nau, *Angew. Chemie - Int. Ed.*, 2015, **54**, 6852–6856.
- 24 E. Leontidis, *Curr. Opin. Colloid Interface Sci.*, 2016, **23**, 100–109.
- 25 E. Leontidis, M. Christoforou, C. Georgiou and T. Delclos, *Curr. Opin. Colloid Interface Sci.*, 2014, **19**, 2–8.
- 26 L. Pérez-Fuentes, C. Drummond, J. Faraudo and D. Bastos-González, *Soft Matter*, 2017, **13**, 1120–1131.
- 27 L. Pérez-Fuentes, C. Drummond, J. Faraudo and D. Bastos-González, *Soft Matter*, 2015, **11**, 5077–5086.
- 28 L. Yang, Y. Fan and Y. Q. Gao, *J. Phys. Chem. B*, 2011, **115**, 12456–12465.
- 29 R. Scheu, B. M. Rankin, Y. Chen, K. C. Jena, D. Ben-Amotz and S. Roke, *Angew. Chemie Int. Ed.*, 2014, **53**, 9560–9563.
- 30 T. López-León, M. J. Santander-Ortega, J. L. Ortega-Vinuesa and D. Bastos-González, *J. Phys. Chem. C*, 2008, **112**, 16060–16069.
- 31 J. M. Peula-García, J. L. Ortega-Vinuesa and D. Bastos-González, *J. Phys. Chem. C*, 2010, **114**, 11133–11139.
- 32 H. G. Schild and D. A. Tirrell, *J. Phys. Chem.*, 1990, **94**, 4352–4356.
- 33 E. Thormann, *RSC Adv.*, 2012, **2**, 8297.
- 34 Y. Zhang, S. Furryk, D. E. Bergbreiter and P. S. Cremer, *J. Am. Chem. Soc.*, 2005, **127**, 14505–14510.
- 35 T. López-León, J. L. Ortega-Vinuesa, D. Bastos-González and A. Elaissari, *J. Colloid Interface Sci.*, 2014, **426**, 300–307.
- 36 H. Lai, Q. Chen and P. Wu, *Soft Matter*, 2013, **9**, 3985.
- 37 X. Ye, Y. Ding and J. Li, *J. Polym. Sci. Part B Polym. Phys.*, 2010, **48**, 1388–1393.
- 38 I. Shechter, O. Ramon, I. Portnaya, Y. Paz and Y. D. Livney, *Macromolecules*, 2010, **43**, 480–487.
- 39 P. J. Haines, *Thermal Methods of Analysis*, Springer Netherlands, Dordrecht, 1995.
- 40 R. L. Danley, *Thermochim. Acta*, 2002, **395**, 201–208.
- 41 P. Gill, T. T. Moghadam and B. Ranjbar, *J. Biomol. Tech.*, 2010, **21**, 167–93.
- 42 D. E. Koppel, *J. Chem. Phys.*, 1972, **57**, 4814–4820.
- 43 K. Kubota, S. Fujishige and I. Ando, *Polym. J.*, 1990, **22**, 15–20.



- 44 M. Heskins and J. E. Guillet, 2006, 37–41.
- 45 K. Otake, H. Inomata, M. Konno and S. Saito, *Macromolecules*, 1990, **23**, 283–289.
- 46 Y. Ding, X. Ye and G. Zhang, *Macromolecules*, 2005, **38**, 904–908.
- 47 H. Cheng, L. Shen and C. Wu, *Macromolecules*, 2006, **39**, 2325–2329.
- 48 Y. Marcus, *Biophys. Chem.*, 1994, **51**, 111–127.
- 49 T. López-León, A. Elaïssari, J. L. Ortega-Vinuesa and D. Bastos-González, *ChemPhysChem*, 2007, **8**, 148–156.
- 50 K. B. Rembert, H. I. Okur, C. Hilty and P. S. Cremer, *Langmuir*, 2015, **31**, 3459–3464.
- 51 T. Hoare and R. Pelton, *Langmuir*, 2008, **24**, 1005–1012.
- 52 T. López-León, J. M. López-López, G. Odriozola, D. Bastos-González and J. L. Ortega-Vinuesa, *Soft Matter*, 2010, **6**, 1114.
- 53 H. Du, S. R. Wickramasinghe and X. Qian, *J. Phys. Chem. B*, 2013, **117**, 5090–5101.
- 54 W. McPhee, K. C. Tam and R. Pelton, *J. Colloid Interface Sci.*, 1993, 156, 24–30.
- 55 X. Qiu, C. M. S. Kwan and C. Wu, *Macromolecules*, 1997, **9297**, 6090–6094.

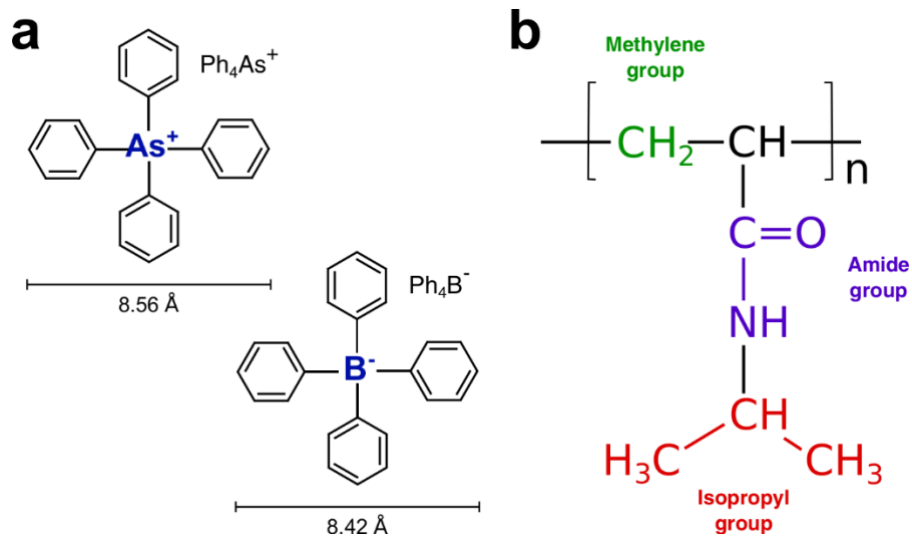


Figure 1: Chemical structures of (a) the tetraphenyl ions (van der Waals diameter is indicated) and (b) the PNIPAM polymer (the different functional groups are shown in different colors)

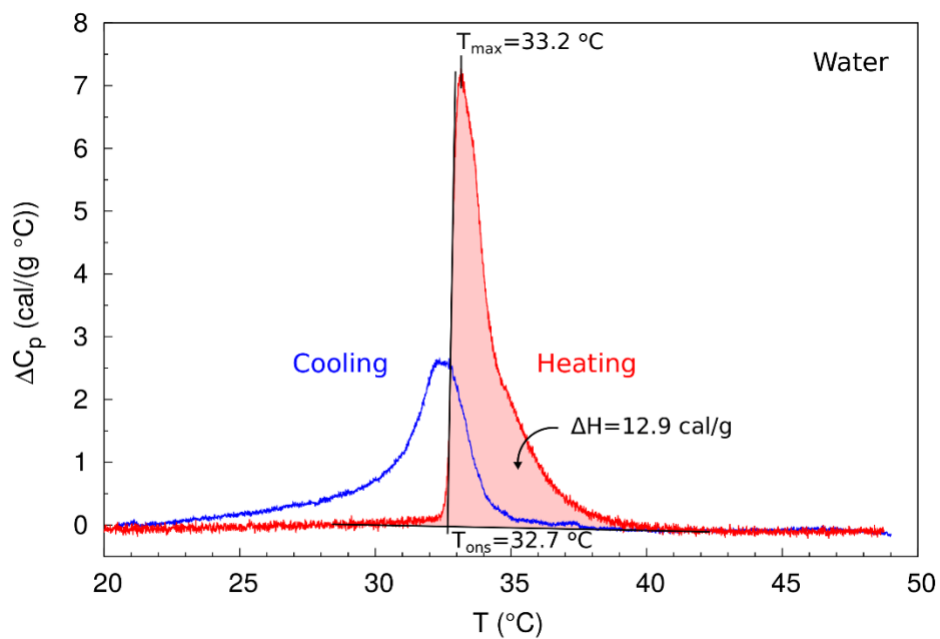


Figure 2: Thermogram of PNIPAM at 15% in pure water for one heating-cooling cycle

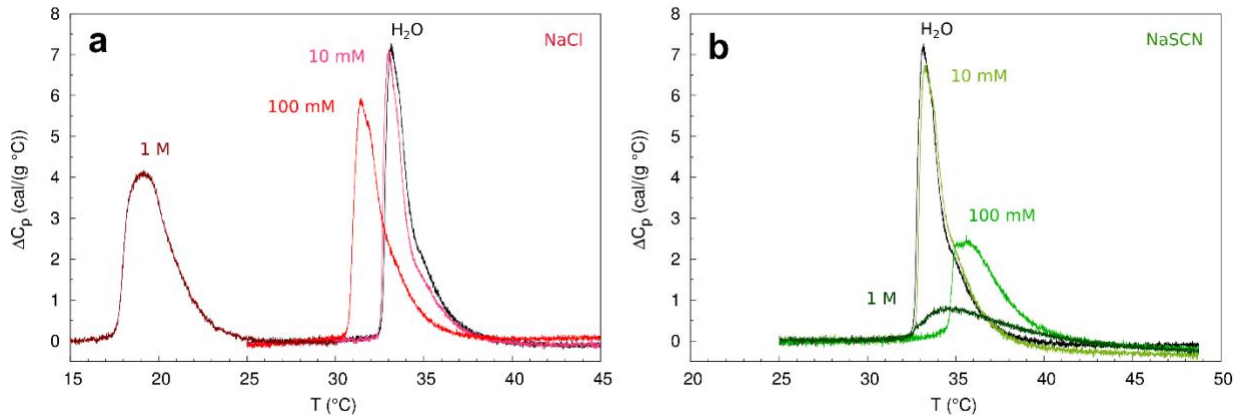


Figure 3: Thermograms of PNIPAM at 15% at different concentrations of (a) NaCl and (b) NaSCN salts. The thermogram in pure water is also shown

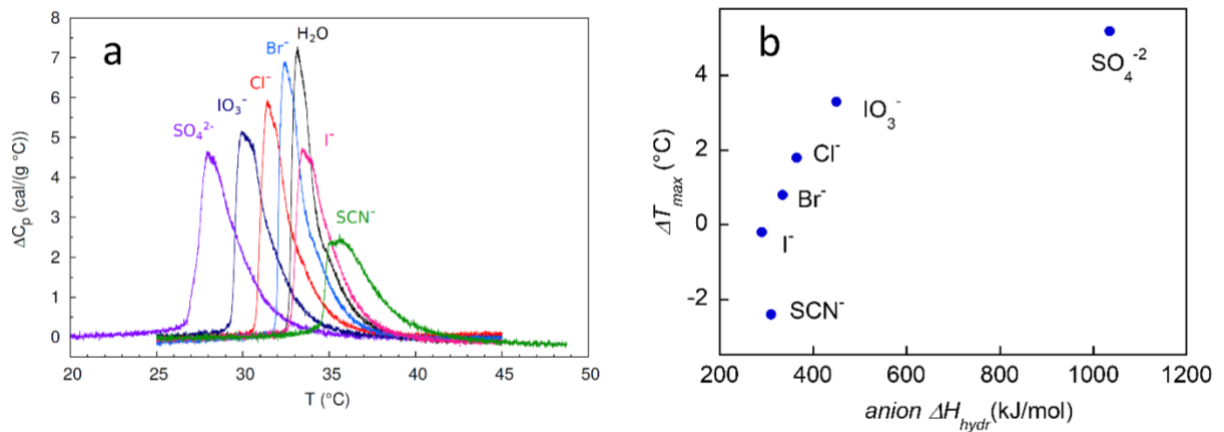


Figure 4: a) Thermograms of PNIPAM at 15% for different salts of the Hofmeister series at 100 mM. The thermogram in pure water is also shown. b)  $\Delta T_{max}$  ( $T_{max}$  (water)- $T_{max}$  (100 mM salt concentration)) vs the hydration enthalpy of the different anions at 298.15K (data from ref. 40)

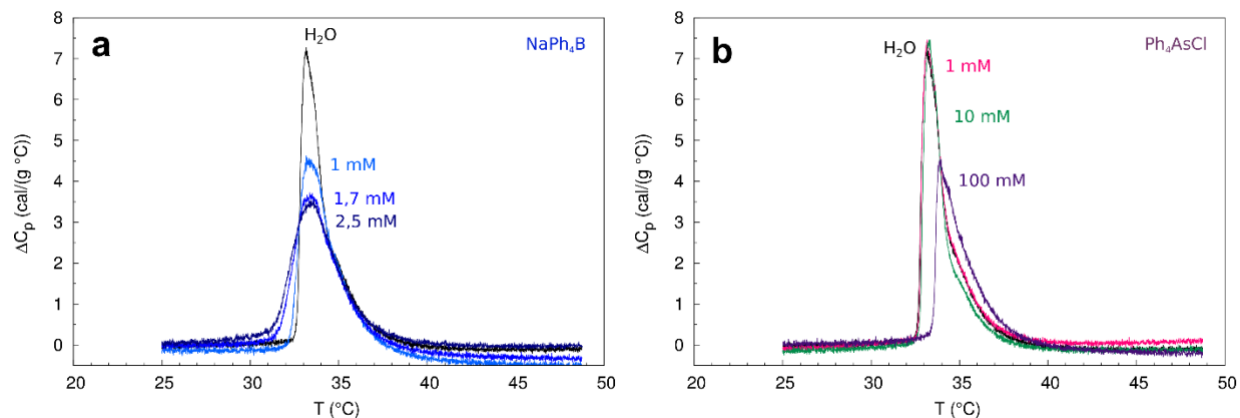


Figure 5: Thermograms of PNIPAM at 15% for the tetraphenyl ions at different concentrations of (a)  $\text{Ph}_4\text{B}^-$  and (b)  $\text{Ph}_4\text{As}^+$ . The thermogram in pure water is also shown

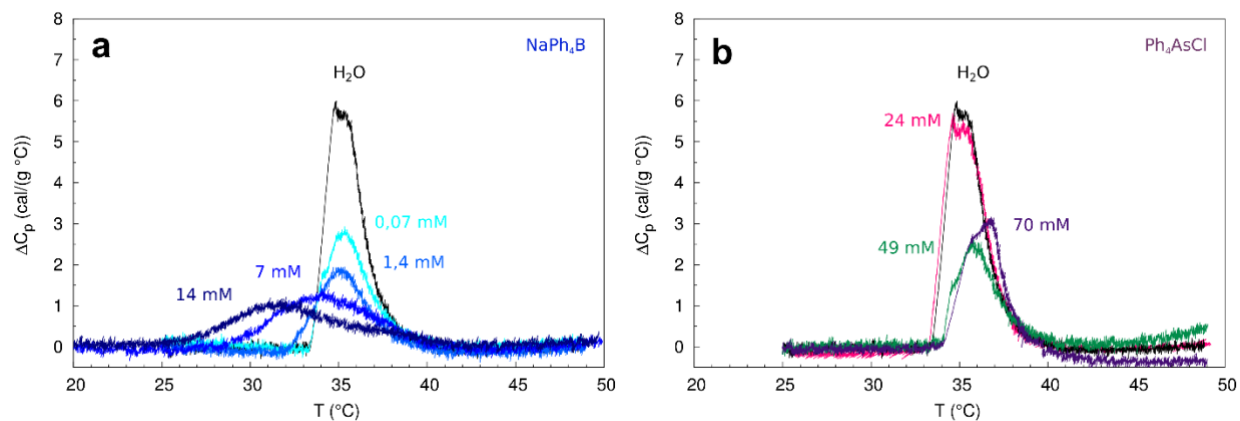


Figure 6: Thermograms of PNIPAM at 5% for the tetraphenyl ions at different concentrations (a)  $\text{Ph}_4\text{B}^-$  (b)  $\text{Ph}_4\text{As}^+$ . The thermogram in pure water is also shown

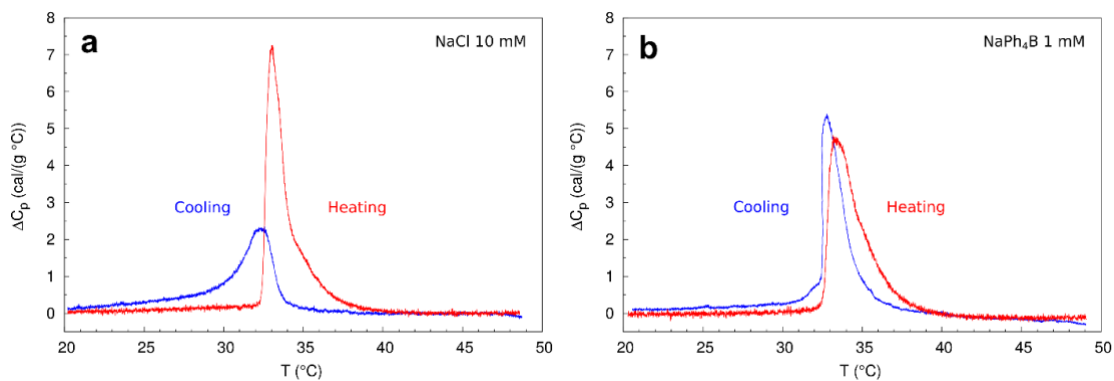


Figure 7: Thermogram of PNIPAM at 15% in solutions of (a) NaCl at 10 mM and (b) NaPh<sub>4</sub>B at 1 mM for one heating-cooling cycle

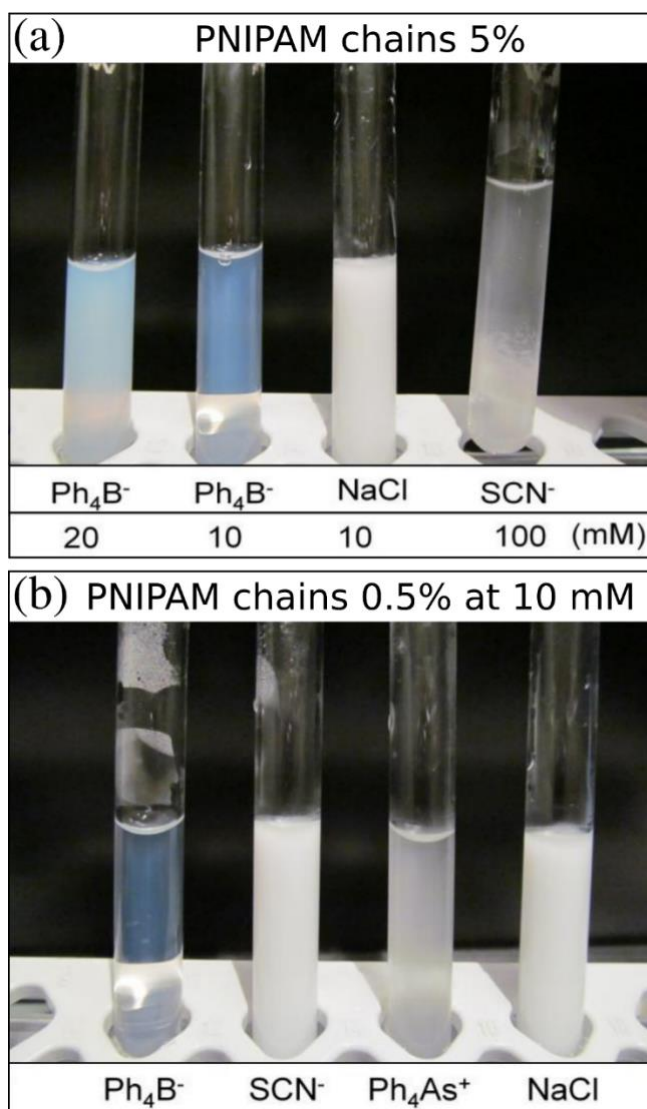


Figure 8: PNIPAM solutions in presence of different salts. PNIPAM concentration (a) 5% (b) 0.5% (10 mM of salt)

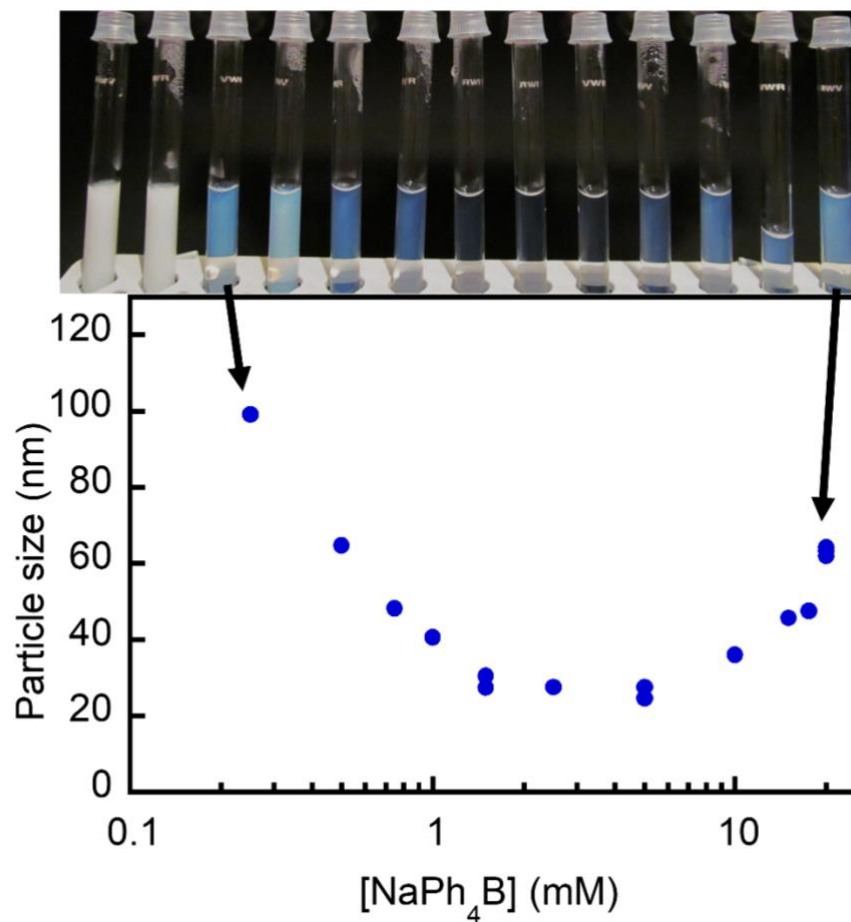


Figure 9: Hydrodynamic diameter of colloidal particles formed upon limited aggregation of PNIPAM in aqueous solutions of different concentrations of  $\text{Ph}_4\text{BNa}$ . T 44°C. PNIPAM concentration 0.5% w/w. Two samples were prepared at each concentration to test reproducibility in particle size. The test tubes photographs, taken at 45°C, clearly evidences the different aggregation state of the PNIPAM/tetraphenyl mixtures

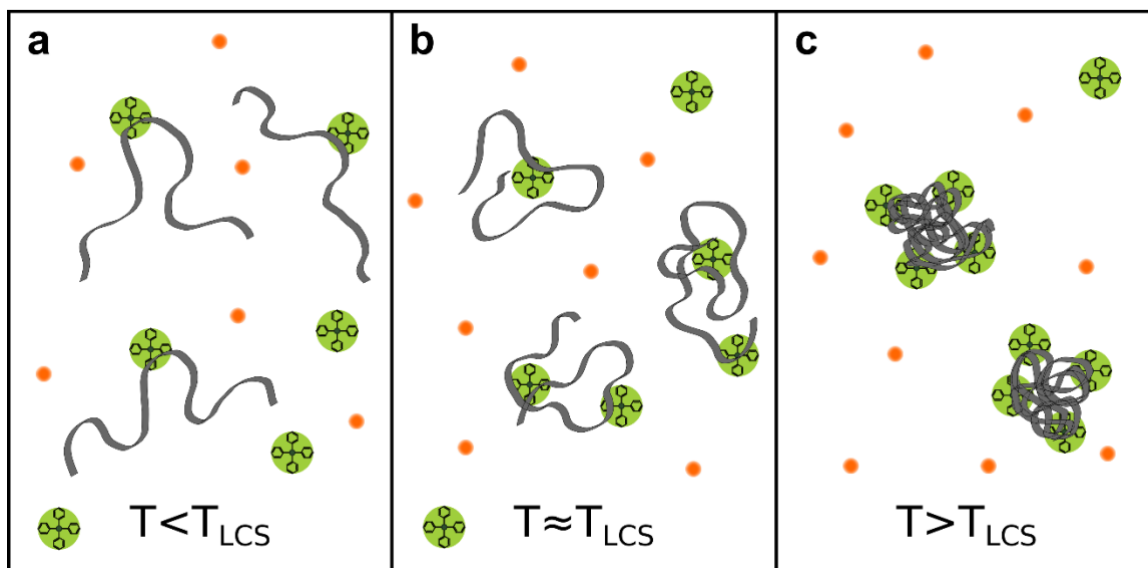


Figure 10: Interaction of tetraphenyl anions and neutral PNIPAM chains at different temperatures: a) Below the  $T_{LCS}$ ,  $\text{Ph}_4\text{B}^-$  ions feel an attraction for the hydrophobic moieties of the hydrated PNIPAM chains; b) Around the  $T_{LCS}$ , the PNIPAM chains begin to dehydrate resulting in a more hydrophobic environment and the tetraphenyl anions increase their interaction with the PNIPAM interface; c) At  $T > T_{LCS}$ , the great adsorption of the anions on PNIPAM chains limits the aggregation of the polymer and produces the formation of monodisperse nanoparticles with electrostatic stability

Table 1:  $T_{LCS}$  and  $T_{max}$  ( $\pm 0.3$  °C) of solutions of PNIPAM at 15% in pure water and in solutions of different salts of the Hofmeister series.

	Water	Na <sub>2</sub> SO <sub>4</sub>	KIO <sub>3</sub>	NaCl	NaBr	NaI	NaSCN
$T_{LCS}$ (°C) [10 mM]	32.7	32.0	31.9	32.6	32.6	32.7	32.8
$T_{max}$ (°C) [10 mM]	33.2	32.6	32.6	33.1	33.1	33.3	33.3
$T_{LCS}$ (°C) [100 mM]	-	27.0	29.4	30.8	32.0	32.8	34.5
$T_{max}$ (°C) [100 mM]	-	28.0	29.9	31.4	32.4	33.4	35.6
$T_{LCS}$ (°C) [1 M]	-	-	-	17.7	-	-	32.0
$T_{max}$ (°C) [1 M]	-	-	-	19.2	-	-	35.0

Table 2: Change in enthalpy ( $\Delta H$ ) ( $\pm 1$  cal/g) of solutions of PNIPAM at 15% in water and in solutions of different salts of the Hofmeister series

Salt concentration	Water	Na <sub>2</sub> SO <sub>4</sub>	KIO <sub>3</sub>	NaCl	NaBr	NaI	NaSCN
10 mM	13	13	13	12	11	13	13
100 mM	13	13	13	12	13	11	8
1 M	13	-	-	14	-	-	6

Table 3:  $T_{LCS}$ ,  $T_{max}$  ( $\pm 0.3$  °C) and enthalpy change ( $\Delta H$ ) of solutions of PNIPAM at 15% in pure water and in solutions of tetraphenyl salts

	Water	NaPh <sub>4</sub> B	NaPh <sub>4</sub> B	NaPh <sub>4</sub> B	Ph <sub>4</sub> AsCl	Ph <sub>4</sub> AsCl	Ph <sub>4</sub> AsCl
		(1mM)	(1.7 mM)	(2.5 mM)	(1mM)	(10mM)	(100mM)
$T_{LCS}$ (°C)	32.7	32.3	31.6	31.3	32.7	32.8	33.5
$T_{max}$ (°C)	33.2	33.2	33.4	33.6	33.2	33.3	33.9
( $\Delta H$ ) ( $\pm 1$ cal/g)	13	11	11	10	12	11	8



Table 4:  $T_{LCS}$ ,  $T_{max}$  ( $\pm 0.3$  °C) and enthalpy change ( $\Delta H$ ) of solutions of PNIPAM at 5% in pure water and in solutions of tetraphenyl salts

	Water	NaPh <sub>4</sub> B (0.07mM)	NaPh <sub>4</sub> B (1.4 mM)	NaPh <sub>4</sub> B (7 mM)	NaPh <sub>4</sub> B (14mM)	Ph <sub>4</sub> AsCl (49mM)	Ph <sub>4</sub> AsCl (70mM)
$T_{LCS}$ (°C)	33.5	33.4	32.5	29.1	26.7	33.9	34.0
$T_{max}$ (°C)	33.9	34.9	34.7	32.8	31.1	35.3	35.3
$(\Delta H)$ ( $\pm 1$ cal/g)	15	9	8	9	8	8	9

# Graphical TOC Entry

